

# The Emergence of Vertical Diversity under Disturbance

Yuya Shishikura\* and Hiroki Ohta†

Department of Human Sciences, Obihiro University of Agriculture and Veterinary Medicine, Hokkaido, 080-8555, Japan

(Dated: January 15, 2024)

We propose a statistical physics model of a neutral community, where each agent can represent identical plant species growing in the vertical direction with sunlight in the form of rich-get-richer competition. Disturbance added to this ecosystem, which makes an agent restart from the lowest growth level, is realized as a stochastic resetting. We show that in this model for sufficiently strong competition, vertical diversity characterized by a family of Hill numbers robustly emerges as a local maximum at intermediate disturbance.

Organisms often compete with other organisms and those could coexist as a whole ecosystem. The theoretical frameworks to understand the mechanism of such coexistence in ecology have been developed based on Lotka-Volterra equation [1]. The developed theories have continued to overcome the obstacles to clarify unexplored coexistence mechanisms [2–12].

One of the important topics in coexistence theory is diversity [13], which is characterized by various indexes such as Hill numbers equivalent to Rényi entropy [14]. Diversity of an ecosystem is largely affected by so-called disturbance [15]. Disturbance is the effects led by the environment outside of an ecosystem, which causes a certain loss of mass of organisms in the ecosystem. There is a qualitative hypothesis that high diversity is achieved at intermediate disturbance, which is called *Intermediate Disturbance Hypothesis* (IDH) [16, 17]. Also, various mathematical models have been found to show what IDH implies [18–23] and a proposal of updating such a hypothesis has been posed [24].

The concept of diversity in ecology is not only used about species, but also used about the spatial structure of an ecosystem such as height of plants [25]. This structural diversity has been discussed in strong relation to species diversity [26, 27]. Indeed, in European forests, structural diversity in terms of canopy height, which is so-called vertical diversity, has been discovered to get the highest at an intermediate disturbance [28]. Also, theoretical models have been developed, focusing on height statistics of plants [29–36]. Nevertheless, IDH in terms of vertical diversity has been hardly mentioned from the perspective of such theoretical models.

In this letter, we develop a theoretical framework of statistical physics models, where one can quantitatively investigate the relationship among competition, disturbance, and vertical diversity in a community of identical species.

The approach taken hereafter can be also regarded as a proposal on a new branch of neutral theories in community ecology [37–40]. Indeed, it has been already discussed how theoretical development can go beyond neutral theories [41] and how the neutral theories ignoring spatially heterogeneous effects can be extended to include such spatial effects [42]. Concretely, let us consider com-

petition among plants for sunlight, which often takes the form of competition such that taller plants are more likely to occupy sunlight and then to get taller. This so-called rich-get-richer form of competition [43] can be *neutral* in the sense that the competition rule is independent of individual plant species.

*Model.*—As preliminaries, suppose that for a given height distribution of plants, we classify it into 3 height levels by putting two thresholds of the average plus or minus standard deviation. Specifically, let  $N \in \mathbb{Z}$  be the total number of agents,  $i \in \{1, \dots, N\}$  be a name of each agent, and  $x_i \in \{1, 2, 3\}$  be the state as the relative height of agent  $i$ . We use a notation  $\mathbf{x} := (x_1, x_2, \dots, x_N) \in \{1, 2, 3\}^N$  as a state of the whole system.

Based on the above considerations, we introduce a stochastic process where the transition rate representing rich-get-richer competition is induced by a simple energy function  $E(\mathbf{x})$ . For simplicity, the energy function is required to have the following two conditions; i) The energy is invariant in terms of replacing the state of maximum 3 by the state of minimum 1 in the whole system:  $E(\mathbf{x}) = E(\mathbf{x}')$  for  $x'_i = -(x_i - 2) + 2$ . ii) In the configuration achieving the minimum energy, the number of state 2 is zero and also the number of state 3 minus the number of state 1 is either zero or  $\pm 1$ . Under these two conditions, we consider the following energy function  $E(\mathbf{x})$  in which each agent interacts with agents at neighboring sites determined by the edges of a graph  $\mathcal{G}$ :

$$E(\mathbf{x}) := -\frac{1}{N} \sum_{i \in V(\mathcal{G})} \sum_{j \in B_i(\mathcal{G})} (x_i - x_j)^2, \quad (1)$$

where  $V(\mathcal{G})$  is the set of all sites in graph  $\mathcal{G}$  and  $B_i(\mathcal{G})$  for  $1 \leq i \leq N$  is the set of all the nearest neighbor sites of site  $i$ .

Indeed, this energy function (1) satisfies i). Further, (1) satisfies ii) because the minimum value of the energy  $-2N$  at the leading order of  $N$  is realized when  $x_i = 1$  or 3 for any  $i$  on the condition that the number of state 1 minus the number of state 3 is either 0 for even  $N$  or  $\pm 1$  for odd  $N$ . For simplicity, we focus on only the case that  $\mathcal{G}$  is the complete graph having edges by which any pair of two sites is directly connected.

Next, let us define  $f_i^\pm$  such that  $f_i^\pm \mathbf{x} := (x_j \pm \delta_{i,j})_{j=1}^N$

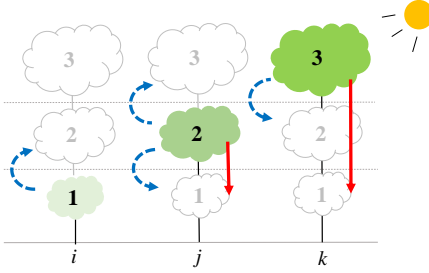


FIG. 1: Schematic diagram for the transition rules between two states for the case of three plants  $i, j, k$ . Under light competition, the transitions from  $x_j = 2$  to 3 or 1 and the reverse transitions as described by dotted blue arrows may occur. Due to disturbance, the transitions from  $x_k = 3$  and  $x_j = 2$  to 1 described as filled red arrows may occur.

for only the case that  $1 \leq f_i^\pm x_i \leq 3$ , where  $\delta_{i,j}$  is the Kronecker delta with  $\delta_{a,b} = 1$  for  $a = b$ , otherwise 0. Then, we introduce a Markov process in continuous time  $t$  as follows. Let us consider a transition rate  $T_0(\mathbf{x} \rightarrow f_i^\pm \mathbf{x})$  from  $\mathbf{x}$  to  $f_i^\pm \mathbf{x}$  is

$$T_0(\mathbf{x} \rightarrow f_i^\pm \mathbf{x}) = \frac{1}{4} \left[ 1 + \tanh \left( -\frac{1}{2} \beta \Delta E(\mathbf{x} \rightarrow f_i^\pm \mathbf{x}) \right) \right], \quad (2)$$

where  $0 \leq \beta$  and  $\Delta E(\mathbf{x} \rightarrow f_i^\pm \mathbf{x}) := E(f_i^\pm \mathbf{x}) - E(\mathbf{x})$

$$= 2 \left\{ \mp 2 \left( x_i - \frac{1}{N} \sum_{i \neq j} x_j \right) - 1 \right\}. \quad (3)$$

*Stochastic resetting as disturbance.*—Next, as a disturbance added to this system, we consider a transition from the current state of an agent to its lowest growth state. This transition can be regarded as one class of stochastic resetting [44]. Concretely, let us consider stochastic resetting from state  $x_i$  to state 1 with a disturbance rate  $R(\mathbf{x} \rightarrow d_i \mathbf{x})$  where  $d_i \mathbf{x} := (x_j (1 - \delta_{i,j}) + \delta_{i,j})_{j=1}^N$  in the following manner:

$$R(\mathbf{x} \rightarrow d_i \mathbf{x}) = r, \quad (4)$$

where  $0 \leq r \leq 1$ .

Combining this stochastic resetting with the above Markov process representing competition, the transition rate  $T(\mathbf{x} \rightarrow \mathbf{x}')$  of the stochastic process that we consider, as schematically illustrated in Fig. 1, is totally

$$\begin{aligned} T(\mathbf{x} \rightarrow \mathbf{x}') = & (1-r) \sum_{1 \leq i \leq N} \sum_{s=\pm} \delta_{\mathbf{x}', f_i^s \mathbf{x}} T_0(\mathbf{x} \rightarrow f_i^s \mathbf{x}) \\ & + \sum_{1 \leq i \leq N} \delta_{\mathbf{x}', d_i \mathbf{x}} R(\mathbf{x} \rightarrow d_i \mathbf{x}). \end{aligned} \quad (5)$$

Next, let  $P_t(\mathbf{x})$  be the probability that the state is  $\mathbf{x}$  at time  $t$ . Then, transition rate (5) leads to the following master equation:

$$\frac{dP_t(\mathbf{x})}{dt} = \sum_{\mathbf{x}' \neq \mathbf{x}} \left( P_t(\mathbf{x}') T(\mathbf{x}' \rightarrow \mathbf{x}) - P_t(\mathbf{x}) T(\mathbf{x} \rightarrow \mathbf{x}') \right). \quad (6)$$

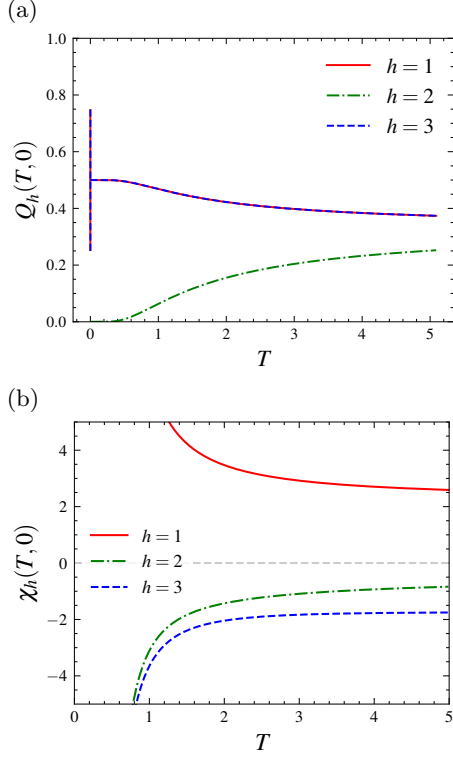


FIG. 2: (a) The density  $Q_h^*(T, 0)$  and (b)  $r$ -susceptibility  $\chi_h(T, 0)$  at  $r = 0$  as a function of  $T$ .

The stationary distribution  $P_{\text{st}}(\mathbf{x})$  is defined such that  $P_t(\mathbf{x}) = P_{\text{st}}(\mathbf{x})$  leads to  $\frac{dP_t(\mathbf{x})}{dt} = 0$ .

Indeed, the canonical distribution  $P_{\text{can}}(\mathbf{x}) := \frac{1}{Z_N(\beta)} \exp(-\beta E(\mathbf{x}))$ , where  $Z_N(\beta) = \sum_{\mathbf{x}} \exp(-\beta E(\mathbf{x}))$ , satisfies the following detailed balanced condition  $P_{\text{can}}(\mathbf{x}) T_0(\mathbf{x} \rightarrow f_i^\pm \mathbf{x}) = P_{\text{can}}(f_i^\pm \mathbf{x}) T_0(f_i^\pm \mathbf{x} \rightarrow \mathbf{x})$ . Hence, the canonical distribution is the stationary distribution satisfying equation (6) with  $r = 0$ .

If disturbance rate holds  $r > 0$ , this stochastic process involves irreversible processes caused by disturbance, because the transition from state 1 to state 3 does not exist but the reverse exists. Thus, the detailed balanced condition can not be satisfied under the presence of disturbance, meaning that  $P_{\text{st}}(\mathbf{x})$  no longer follows the canonical distribution determined by the energy function (1).

*Derivation of population dynamics.*—Although the master equation has the complete information about the stationary distribution, in order to avoid dealing with  $3^N$  states, we consider the time evolution of the density of each of three different states in the limit of large  $N$ . We show how to derive such a set of closed equations in the following.

First, let  $Q_h$  be the density of state  $h \in \{1, 2, 3\}$ , and be  $\mathbf{Q} := (Q_1, Q_2, Q_3) \in [0, 1]^3$ . Then we focus on the transition rate  $U(h \rightarrow h \pm 1 | \mathbf{Q})$  from state  $h$  to  $h \pm 1 \in \{1, 2, 3\}$  of an agent for given  $\mathbf{Q}$  in the limit of large  $N$ . Taking into account (2) and (3),  $U$  turns out to be equal

to

$$\frac{(1-r)}{4} \left[ 1 + \tanh \left( -\beta \Delta e_{\pm} (h | \mathbf{Q}) \right) \right], \quad (7)$$

where

$$\Delta e_{\pm} (h | \mathbf{Q}) = \left\{ \mp 2 \left( h - \sum_{h'=1}^3 h' Q_{h'} \right) - 1 \right\}. \quad (8)$$

Note that it is assumed that the replacement of  $\sum_{i \neq j} x_i/N$  by  $\sum_{h'=1}^3 h' Q_{h'}$  in the limit of  $N \rightarrow \infty$  holds, which can be regarded as self-averaging. Taking into account disturbance rate (4), the time evolution of each density  $Q_h$  for  $h = 1$  and 3 is exactly described as  $\frac{dQ_h}{dt} = V_h(\mathbf{Q})$ , which is explicitly:

$$\begin{aligned} \frac{dQ_h}{dt} = & -\delta_{h,3} r Q_3 + Q_2 U(2 \rightarrow h | \mathbf{Q}) \\ & + \delta_{h,1} r \sum_{h'=2}^3 Q_{h'} - Q_h U(h \rightarrow 2 | \mathbf{Q}). \end{aligned} \quad (9)$$

*Densities and susceptibility in stationary states.*—Let us compute the stationary solutions of the derived population dynamics (9). The density of each state  $h$  in a stationary solution satisfying  $V_h(\mathbf{Q}^*) = 0$  is described by  $Q_h^*(T, r)$  as a function of two parameters of  $T = \beta^{-1}$  and  $r$ . Note that because of  $Q_1^* + Q_2^* + Q_3^* = 1$ , we have  $Q_2^* = 1 - Q_1^* - Q_3^*$  and also  $\sum_{h=1}^3 h Q_h^* = -Q_1^* + Q_3^* + 2$ , by which equation (9) are written as two coupled equations depending on only  $Q_1^*$  and  $Q_3^*$ .

Let us consider the case of  $r = 0$  for any  $T$ . As shown in Fig. 2(a), it turns out that there is a symmetric solution  $Q_1^*(T, 0) = Q_3^*(T, 0) = (2 + \exp(-2\beta))^{-1}$ . At  $T = 0$ , in addition to this symmetric solution, we obtain the other asymmetric solutions as follows:

$$\frac{1}{4} < Q_1^*(0, 0) = 1 - Q_3^*(0, 0) < \frac{3}{4}. \quad (10)$$

Next, let us consider a response of the density against  $r$  around  $r \ll 1$ , which is characterized by  $r$ -susceptibility  $\chi_h(T, r) := \frac{\partial Q_h^*}{\partial r}$  for any  $h$ . As shown in Fig. 2(b), using Taylor series expansion, we straightforwardly obtain

$$\begin{aligned} \chi_1(T, 0) &= 4 \frac{(2 + g_{\beta})(4 + g_{\beta}^2) + 4g'_{\beta}\beta(2 - g_{\beta})}{(2 + g_{\beta})^2((2 + g_{\beta})(2 - g_{\beta}) + 8g'_{\beta}\beta)}, \\ \chi_3(T, 0) &= 4 \frac{-4g_{\beta}(2 + g_{\beta}) + 4g'_{\beta}\beta(2 - g_{\beta})}{(2 + g_{\beta})^2((2 + g_{\beta})(2 - g_{\beta}) + 8g'_{\beta}\beta)}, \end{aligned} \quad (11)$$

where  $g_{\beta} = 1 + \tanh \beta$  with  $g_0 = 1 \leq g_{\beta} < 2 = \lim_{\beta \rightarrow \infty} g_{\beta}$  and  $g'_{\beta} = (\cosh \beta)^{-2}$ . Note that  $\chi_2 = -\chi_1 - \chi_3$  by definition. It is notable that  $\chi_h$  for each  $h$  shows an exponential divergence as  $\beta \rightarrow \infty$ .

Let us move onto the case of  $T \ll 1$  for any  $r > 0$ . Similar to the case with  $r = 0$ , we consider a response of the density against  $T$  around  $T \ll 1$ , which is characterized

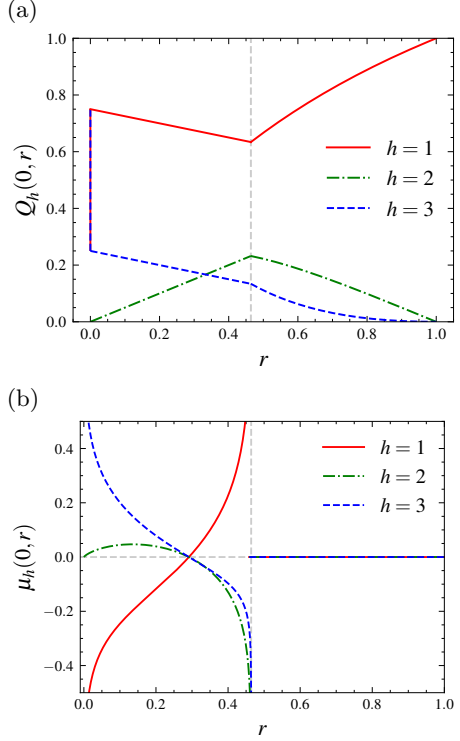


FIG. 3: (a) The density  $Q_h^*(0, r)$  and (b)  $T$ -susceptibility  $\mu_h(0, r)$  as a function of disturbance rate  $r$ .

by  $T$ -susceptibility  $\mu_h(T, r) := \frac{\partial Q_h^*}{\partial T}$  for any  $h$ . As shown in Fig. 3, those in the limit of  $T \rightarrow 0$  are computed in the following. First, for  $r_0 = -3 + 2\sqrt{3} < r \leq 1$ , we obtain

$$\begin{aligned} Q_1^*(0, r) &= \frac{2r}{1+r}, \\ Q_3^*(0, r) &= \frac{(1-r)^2}{(1+r)^2}, \end{aligned} \quad (12)$$

and  $\mu_h(0, r) = 0$  for any  $h$ .

For  $0 < r < r_0$ , it is rather tricky that  $Q_1^*(0, r)$  can not be exactly computed solely. In order to compute  $Q_1^*(0, r)$ , one can perform Taylor series expansion as  $Q_1^*(T, r) = Q_1^*(0, r) + \mu_1(0, r)T + O(T^2)$  and then substitute it into equation (9). Assuming that all the terms for each order with respect to  $T$  separately satisfy equation (9), we finally obtain

$$Q_1^*(0, r) = Q_3^*(0, r) + \frac{1}{2} = -\frac{1}{4}r + \frac{3}{4}, \quad (13)$$

$$\mu_1(0, r) = -\frac{1+r}{1-r}\mu_3(0, r) = -\frac{1+r}{4}\text{artanh } \theta(r), \quad (14)$$

where  $\theta(r) = (-r^2 - 10r + 3)/(1 - r)(3 + r)$ . Note that  $\lim_{r \rightarrow r_0} \theta(r) = -1 < \theta(r) < 1 = \lim_{r \rightarrow 0} \theta(r)$  for  $0 < r < r_0$ , and  $\mu_2 = -\mu_1 - \mu_3$  by definition. It is notable that  $\mu_h$  for  $h = 1, 3$  as  $r \rightarrow 0$  and for any  $h$  as  $r \rightarrow r_0$  show logarithmic divergences. Further, finite size fluctuations have been found to show distinct behaviors between lower  $r$  and higher  $r$  compared to  $r_0$  (See Supplemental Material).

For  $T \rightarrow \infty$ , we can straightforwardly obtain the analytical form of  $Q_h^*(\infty, r)$  and  $\chi_h(\infty, r)$ , which satisfies  $\chi_1 > 0, \chi_2 < 0, \chi_3 < 0$ , and  $Q_1^* > Q_2^*, Q_3^*$  for any  $r > 0$  (See Supplemental Material). Note that  $\nu_h(\infty, r) := \frac{\partial Q_h^*}{\partial \beta} = 0$  holds for any  $h$ .

*Diversity indexes.*—Let us focus on Hill numbers for  $\alpha > 0$  and  $\alpha \neq 1$ :

$$D_\alpha := \left( \sum_{h=1}^3 Q_h^\alpha \right)^{1/(1-\alpha)}, \quad (15)$$

which satisfies the replication principle [14] and quantifies the vertical diversity of the model with  $1 \leq D_\alpha \leq 3$ . Further, we define  $D_1 := \lim_{\alpha \rightarrow 1} D_\alpha = \exp(-\sum_{h=1}^3 Q_h^* \log Q_h^*)$ , equivalent to the exponential of Shannon entropy.

In Fig. 4(a),  $D_\alpha$  for  $\alpha = 0.1, 1, 10, 100$  are shown at  $T = 0$ . Those diversity indexes robustly get a maximum as a function of single variable  $r$  at an intermediate disturbance  $r = r_0$  for  $\alpha \geq 0.199$ . Note that the maximum points for  $\alpha \leq 0.198$  get less than  $r_0$ , which converge to  $r = 0.451 \dots < r_0$  as  $\alpha \rightarrow 0$ .

As shown on the  $(T, r)$ -parameter plane in Fig. 4(b), whereas  $r = 0$  could get also the local or global maximum point for any  $T > 0$ , local maximum points  $r_\ell(T, \alpha) > 0$  of  $D_\alpha$  as a function of single variable  $r$  are determined by  $\partial_r D_\alpha(r_\ell(T, \alpha)) = 0$ . Indeed, there is a point around  $T = 0.25$  below which there exists robustly a local maximum point for any  $\alpha > 0$ . On the contrary, for  $T \geq 0.26$ ,  $r_\ell(T, \alpha)$  does not exist for all the values of  $\alpha$  higher than a sufficiently large  $\alpha_0(T)$ .

Related to this phenomenon, we have also found that the local minima of  $Q_1^*$  as a function of single variable  $r$ , which are observed for  $T \leq 0.25$ , disappear for  $T \geq 0.26$ . The absence of local maxima of  $D_\alpha$  for any  $\alpha > 0$  is analytically confirmed on the condition that  $\chi_1 > 0, \chi_2 < 0, \chi_3 < 0$ , and  $Q_1^* > Q_2^*, Q_3^*$  hold for any  $r > 0$  corresponding to, at least, the case with  $T \rightarrow \infty$  where  $\alpha_0(\infty) = 0$  (See Supplemental Material). Further, the local maxima of  $Q_2$  exist for  $T \leq 2.58$ , it seems to disappear between  $T = 2.58$  and  $T = 2.60$ , which is very close to the lower limit of the absence of local maxima of  $D_\alpha$  for any  $\alpha$ .

*Concluding remarks.*—In this letter, we have proposed a neutral community model of identical plant species with rich-get-richer competition, which robustly exhibit emergent vertical diversity that has a local maximum at an intermediate disturbance for sufficient strong competition.

The proposed neutral model can be easily generalized into a non-neutral model with multiple species by introducing species dependence into transition rates representing competition or disturbance. In another direction, one can study spatial effects by considering the model on finite-dimensional lattice such as one-dimensional

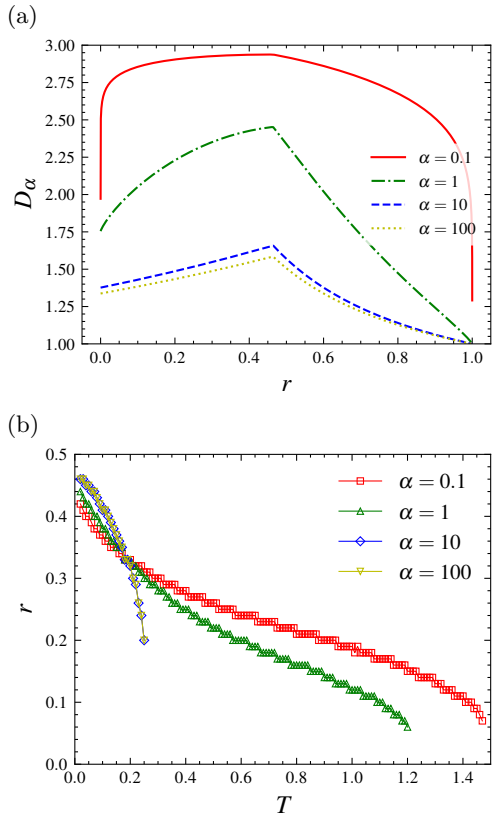


FIG. 4: (a) Diversity indexes  $D_\alpha(r)$  for  $Q_h^*$  at  $T \rightarrow 0$ .  $\alpha = 0.1, 1, 10, 100$ . (b) The local maximum points  $r_\ell(T, \alpha)$  of  $D_\alpha(r)$  depending on  $(T, \alpha)$  for  $Q_h^*$ .  $r_\ell(0, 0.1) = 0.457 \dots < r_0 = 0.464 \dots$ . The data points of  $r_\ell(T, \alpha)$  are estimated within the numerical resolution by a nullcline method where the increment of  $r$  and  $T$  is  $10^{-2}$ .

chain instead of the complete graph. Based on finite-dimensional lattice models, a mixing process can be also introduced as a parameter to study how such lattice models go through a transition to the corresponding population dynamics such as Lotka-Volterra type of equation [45]. The relationship between lattice models and population dynamics is one topic discussed in the context of intermediate disturbance hypothesis [22]. Those cases remain to be studied in the future.

*Acknowledgements.*—The authors would like to thank Obihiro University of Agriculture and Veterinary Medicine for providing the facilities to accomplish this work.

\* shishikurayuya@gmail.com

† hiroki@obihiro.ac.jp

- [1] J. Hofbauer and K. Sigmund, *Dynamical Systems and Lotka-Volterra Equations, Evolutionary Games and Population Dynamics* (Cambridge University Press, Cambridge, 1998), pp. 1–54.
- [2] D. Tilman, *Resource competition and community struc-*

ture (Princeton University Press, Princeton, 1982).

[3] P. Chesson, General theory of competitive coexistence in spatially-varying environments, *Theor. Popul. Biol.* **58**, 211 (2000).

[4] D. A. Kessler and N. M. Shnerb, Generalized model of island biodiversity, *Phys. Rev. E* **91**, 042705 (2015).

[5] T. Obuchi, Y. Kabashima, and K. Tokita, Multiple peaks of species abundance distributions induced by sparse interactions, *Phys. Rev. E* **94**, 022312 (2016).

[6] M. Tikhonov and R. Monasson, Collective Phase in Resource Competition in a Highly Diverse Ecosystem, *Phys. Rev. Lett.* **118**, 048103 (2017).

[7] G. Bunin, Ecological communities with Lotka-Volterra dynamics, *Phys. Rev. E* **95**, 042414 (2017).

[8] G. Biroli, G. Bunin, and C. Cammarota, Marginally Stable Equilibria in Critical Ecosystems, *New J. Phys.* **20**, 083051 (2018).

[9] W. Cui, R. Marsland III, and P. Mehta, Effect of Resource Dynamics on Species Packing in Diverse Ecosystems, *Phys. Rev. Lett.* **125**, 048101 (2020).

[10] D. Gupta, S. Garlaschi, S. Suweis, S. Azaele, and A. Maritan, Effective resource competition model for species coexistence, *Phys. Rev. Lett.* **127**, 208101 (2021).

[11] M. Barbier, C. de Mazancourt, M. Loreau, and G. Bunin, Fingerprints of High-Dimensional Coexistence in Complex Ecosystems, *Phys. Rev. X* **11**, 011009 (2021).

[12] V. Ros, F. Roy, G. Biroli, G. Bunin, and A. M. Turner, Generalized Lotka-Volterra Equations with Random, Nonreciprocal Interactions: The Typical Number of Equilibria, *Phys. Rev. Lett.* **130**, 257401 (2023).

[13] A. E. Magurran and B. J. McGill, (Eds.) *Biological diversity: frontiers in measurement and assessment* (Oxford University Press, Oxford, 2010).

[14] T. Leinster, *Entropy and diversity: the axiomatic approach* (Cambridge University Press, Cambridge, 2021).

[15] M. L. Viljuri, et al, The effect of natural disturbances on forest biodiversity: an ecological synthesis, *Biol. Rev.* **97**, 1930 (2022).

[16] J. P. Grime, Competitive exclusion in herbaceous vegetation, *Nature* **242**, 344 (1973).

[17] J. H. Connell, Diversity in tropical rain forests and coral reefs: high diversity of trees and corals is maintained only in a nonequilibrium state, *Science* **199**, 1302 (1978).

[18] P. S. Petraitis, R. E. Latham, and R. A. Niesenbaum, The maintenance of species diversity by disturbance, *Q. Rev. Biol.* **64**, 393 (1989).

[19] H. Caswell and J. E. Cohen, Disturbance, interspecific interaction and diversity in metapopulations, *Biol. J. Linn. Soc.* **42**, 193 (1991).

[20] M. Kondoh, Unifying the relationships of species richness to productivity and disturbance, *Proc. R. Soc. B* **268**, 269 (2001).

[21] S. H. Roxburgh, K. Shea, and J. B. Wilson, The intermediate disturbance hypothesis: patch dynamics and mechanisms of species coexistence, *Ecology* **85**, 359 (2004).

[22] J. R. Svensson, M. Lindegarth, P. R. Jonsson, and H. Pavia, Disturbance–diversity models: what do they really predict and how are they tested?, *Proc. R. Soc. B* **279**, 2163 (2012).

[23] R. Hunt and R. L. Colasanti, Real communities of virtual plants explain biodiversity on just three assumptions, *in silico Plants* **3**, diab015 (2021).

[24] J. W. Fox, The intermediate disturbance hypothesis should be abandoned, *Trends Ecol. Evol.* **28**, 86 (2013).

[25] J. F. Franklin, et al., Disturbances and structural development of natural forest ecosystems with silvicultural implications, using Douglas-fir forests as an example, *For. Ecol. Manag.* **155**, 399 (2002).

[26] A. Inoue and S. Yoshida, Forest stratification and species diversity of *Cryptomeria japonica* natural forests on Yakushima, *J. for. plan.* **7**, 1 (2001).

[27] M. Ehbrecht, D. Seidel, P. Annighöfer, H. Kreft, M. Köhler, D. C. Zemp, and C. Ammer, Global patterns and climatic controls of forest structural complexity, *Nat. Commun.* **12**, 519 (2021).

[28] C. Senf, A. S. Mori, J. Müller, and R. Seidl, The response of canopy height diversity to natural disturbances in two temperate forest landscapes, *Landsc. Ecol.* **35**, 2101 (2020).

[29] T. Hara, A stochastic model and the moment dynamics of the growth and size distribution in plant populations, *J. Theor. Biol.* **109**, 173 (1984).

[30] M. Yokozawa, Size hierarchy and stability in competitive plant populations, *Bull. Math. Biol.* **61**, 949 (1999).

[31] M. A. Zavala, Ó. Angulo, R. B. de la Parra, and J. C. López-Marcos, An analytical model of stand dynamics as a function of tree growth, mortality and recruitment: The shade tolerance-stand structure hypothesis revisited. *J. Theor. Biol.* **244**, 440 (2007).

[32] N. Strigul, D. Pristinski, D. Purves, J. Dushoff, and S. Pacala, Scaling from trees to forests: tractable macroscopic equations for forest dynamics, *Ecol. Monogr.* **78**, 523 (2008).

[33] D. W. Purves, J. W. Lichstein, N. Strigul, and S. W. Pacala, Predicting and understanding forest dynamics using a simple tractable model, *Proc. Natl. Acad. Sci. U.S.A.* **105**, 17018 (2008).

[34] T. Kohyama, and T. Takada The stratification theory for plant coexistence promoted by one-sided competition, *J. Ecol.* **97**, 463 (2009).

[35] M. Cammarano, Co-dominance and succession in forest dynamics: the role of interspecific differences in crown transmissivity, *J. Theor. Biol.* **285**, 46 (2011).

[36] T. S. Kohyama and T. Takada, One-sided competition for light promotes coexistence of forest trees that share the same adult height, *J. Ecol.* **100**, 1501 (2012).

[37] R. H. MacArthur and E. O. Wilson, *The theory of Island Biogeography. Monographs in Population Biology* (Princeton University Press, Princeton, 1967).

[38] H. Caswell, Community structure: a neutral model analysis, *Ecol. Monogr.* **46**, 327 (1976).

[39] S. P. Hubbell, *The Unified Neutral Theory of Biodiversity and Biogeography* (Princeton University Press, Princeton, 2001).

[40] I. Volkov, J. R. Banavar, S. P. Hubbell, and A. Maritan, Neutral theory and relative species abundance in ecology, *Nature* **424**, 1035 (2003).

[41] S. Azaele, S. Suweis, J. Grilli, I. Volkov, J. R. Banavar, Statistical mechanics of ecological systems: Neutral theory and beyond, *Rev. Mod. Phys.* **88**, 035003 (2016).

[42] S. Pigolotti, M. Cencini, D. Molina, and M. A. Muñoz, Stochastic Spatial Models in Ecology: A Statistical Physics Approach, *J. Stat. Phys.* **172**, 44 (2018).

[43] R. K. Merton, The Matthew effect in science, *Science* **159**, 56 (1968).

[44] A. Nagar and G. Shamik, Stochastic resetting in interacting particle systems: a review, *J. Phys. A* **56**, 283001

(2023).

[45] C. W. Feldager, N. Mitarai, and H. Ohta, Deterministic extinction by mixing in cyclically competing species, Phys. Rev. E **95**, 032318 (2017).

# Supplemental Material to "The Emergence of Vertical Diversity under Disturbance"

Yuya Shishikura and Hiroki Ohta

Department of Human Sciences, Obihiro University of Agriculture and Veterinary Medicine, Hokkaido, 080-8555, Japan

(Dated: January 15, 2024)

## I. THE EQUATIONS TO DETERMINE THE STATIONARY SOLUTIONS OF THE POPULATION DYNAMICS

As mentioned in the main text, based on the model we study, we consider  $\mathbf{Q} := (Q_1, Q_2, Q_3) \in [0, 1]^3$  where  $Q_h$  is the density of each state  $h$ . Then, we may derive the following equation of the population dynamics of  $\mathbf{Q}$  for  $h = 1, 3$ :

$$\begin{aligned} \frac{dQ_h}{dt} &= V_h(\mathbf{Q}), \\ V_h(\mathbf{Q}) &= -\delta_{h,3}rQ_3 + Q_2U\left(2 \rightarrow h \mid \mathbf{Q}\right) + \delta_{h,1}r \sum_{h'=2}^3 Q_{h'} - Q_hU\left(h \rightarrow 2 \mid \mathbf{Q}\right). \end{aligned} \quad (1)$$

We define  $Q_h^*$  such that  $V_h(\mathbf{Q}^*) = 0$  holds for  $h = 1, 3$ .

Let us remind that because of  $Q_1^* + Q_2^* + Q_3^* = 1$ , we have

$$Q_2^* = 1 - Q_1^* - Q_3^*, \quad (2)$$

$$\sum_{h=1}^3 hQ_h^* = -Q_1^* + Q_3^* + 2. \quad (3)$$

We substitute (2) and (3) into (1) and then obtain the following for  $h = 1, 3$ :

$$\begin{aligned} &-\delta_{h,3}rQ_3^* + (1 - Q_1^* - Q_3^*)\frac{(1-r)}{4}\left(1 + G_\beta^{(h)}(Q_3^* - Q_1^*)\right) \\ &+ \delta_{h,1}r(1 - Q_1^*) - Q_h^*\frac{(1-r)}{4}\left(1 - G_\beta^{(h)}(Q_3^* - Q_1^*)\right) = 0, \end{aligned} \quad (4)$$

where

$$G_\beta^{(h)}(a) = \tanh \beta \left( (\delta_{h,1} - \delta_{h,3})2a + 1 \right). \quad (5)$$

### A. The explicit expressions of $Q_h^*$ and $\chi_h$ at $r \rightarrow 0$

Based on (4) for  $T > 0$ , we find the stationary solution of the densities  $Q_1^*$  and  $Q_3^*$  satisfying the following:

$$\frac{1}{4}(1 - 2Q_1^*)(1 + \tanh \beta) - \frac{1}{4}Q_1^*(1 - \tanh \beta) = 0. \quad (6)$$

Then, taking into account (2), we obtain

$$\begin{aligned} Q_1^*(T, 0) &= Q_3^*(T, 0) = \frac{1}{2 + \exp(-2\beta)}, \\ Q_2^*(T, 0) &= \frac{\exp(-2\beta)}{2 + \exp(-2\beta)}. \end{aligned} \quad (7)$$

Next, we focus on the case of  $T = 0$  where the following holds:

$$\lim_{T \rightarrow 0} G_\beta^{(h)}(a) = \begin{cases} 1 & \text{if } \beta \left( (\delta_{h,1} - \delta_{h,3})2a + 1 \right) > 0 \\ -1 & \text{if } \beta \left( (\delta_{h,1} - \delta_{h,3})2a + 1 \right) < 0 \\ 0 & \text{if } \beta \left( (\delta_{h,1} - \delta_{h,3})2a + 1 \right) = 0. \end{cases} \quad (8)$$

There are 6 cases in terms of the possibilities of taking values of  $G_\beta^{(1)}(a)$  and  $G_\beta^{(3)}(a)$ , each of which can be  $-1$ ,  $0$ , or  $1$ . Note that if one of  $G_\beta^{(1)}(a)$  and  $G_\beta^{(3)}(a)$  is  $0$ , the value of the other is uniquely determined. Indeed, when the two conditions of

$$\begin{cases} -2Q_1^* + 2Q_3^* + 1 > 0, \\ 2Q_1^* - 2Q_3^* + 1 > 0, \end{cases} \quad (9)$$

hold, based on (4), we obtain

$$Q_3^* = -Q_1^* + 1, \quad (10)$$

where we have used

$$\lim_{T \rightarrow 0} G_\beta^{(h)}(Q_3^* - Q_1^*) = 1, \quad (11)$$

for  $h = 1, 3$ . Additionally, the two conditions of (9) lead to

$$\begin{aligned} \frac{1}{4} < Q_1^*(0, 0) < \frac{3}{4}, \\ Q_3^*(0, 0) &= 1 - Q_1^*(0, 0), \\ Q_2^*(0, 0) &= 0. \end{aligned} \quad (12)$$

Note that the other 5 cases for the possibilities of taking values of  $G_\beta^{(h)}(a)$  give no solutions of equation (4).

In order to compute  $\chi_h(T, r) := \frac{\partial Q_h^*}{\partial r}$  for  $T > 0$ , let us perform Taylor series expansion of  $Q_h^*(T, r)$  at  $r = 0$  for  $h = 1, 3$  as follows:

$$Q_h^*(T, r) = Q_h^*(T, 0) + \chi_h(T, 0)r + O(r^2). \quad (13)$$

Then, substituting this form with (7) into (4), for  $O(\beta r) \ll 1$  up to  $O(r)$  order, we obtain

$$\begin{aligned} -2\chi_1 - g_\beta \chi_3 + \frac{4g'_\beta \beta}{2 + g_\beta} (\chi_3 - \chi_1) + \frac{8}{2 + g_\beta} &= 0, \\ -g_\beta \chi_1 - 2\chi_3 + \frac{4g'_\beta \beta}{2 + g_\beta} (\chi_1 - \chi_3) - \frac{4g_\beta}{2 + g_\beta} &= 0, \end{aligned} \quad (14)$$

where

$$g_\beta = 1 + \tanh \beta, \quad (15)$$

$$g'_\beta = \frac{1}{\cosh^2 \beta}, \quad (16)$$

with  $g_0 = 1 \leq g_\beta < \lim_{\beta \rightarrow \infty} g_\beta = 2$ .

Solving these equations, we finally obtain

$$\begin{aligned} \chi_1(T, 0) &= 4 \frac{(2 + g_\beta)(4 + g_\beta^2) + 4g'_\beta \beta(2 - g_\beta)}{(2 + g_\beta)^2((2 + g_\beta)(2 - g_\beta) + 8g'_\beta \beta)}, \\ \chi_3(T, 0) &= 4 \frac{-4g_\beta(2 + g_\beta) + 4g'_\beta \beta(2 - g_\beta)}{(2 + g_\beta)^2((2 + g_\beta)(2 - g_\beta) + 8g'_\beta \beta)}, \end{aligned} \quad (17)$$

where  $g'_\beta \beta \simeq \beta \exp(-2\beta) \rightarrow 0$  as  $\beta \rightarrow \infty$  and  $g'_\beta \beta \simeq \beta \rightarrow 0$  as  $\beta \rightarrow 0$ . Note that  $\chi_2 = -\chi_1 - \chi_3$  by definition.

## B. The explicit expressions of $Q_h^*$ and $\mu_h$ at $T \rightarrow 0$

Among 6 possibilities of taking values of  $G_\beta^{(1)}$  and  $G_\beta^{(3)}$ , let us consider the situation where the following two conditions hold for  $T \ll 1$ :

$$\begin{cases} -2Q_1^* + 2Q_3^* + 1 = 0, \\ 2Q_1^* - 2Q_3^* + 1 > 0. \end{cases} \quad (18)$$

In this case, we need to take the limit of  $T \rightarrow 0$  carefully. First, we can perform Taylor series expansion of  $Q_h^*(T, r)$  at  $T = 0$  as

$$Q_h^*(T, r) = Z_h + \mu_h(0, r)T + O(T^2), \quad (19)$$

where  $Z_h := Q_h^*(0, r)$  and  $\mu_h(T, r) := \frac{\partial Q_h^*}{\partial T}$ . Substituting this form into (4), we obtain, up to  $O(T^0)$  order,

$$\begin{aligned} & \frac{(1-r)}{4}(1-Z_1-Z_3)\left\{1+\tanh 2(-\mu_1+\mu_3)\right\} \\ & -\frac{(1-r)}{4}Z_1\left\{1-\tanh 2(-\mu_1+\mu_3)\right\}+r(1-Z_1)=0, \end{aligned} \quad (20)$$

$$\frac{1}{2}(1-r)(1-Z_1-Z_3)-rZ_3=0, \quad (21)$$

where the second equation is obtained on the condition of (18) corresponding to

$$\lim_{T \rightarrow 0} G_\beta^{(3)}(Q_3^* - Q_1^*) \rightarrow 1. \quad (22)$$

Combining (21) with the first condition of (18) gives

$$\begin{aligned} Z_1 &= Q_1^*(0, r) = -\frac{1}{4}r + \frac{3}{4}, \\ Z_3 &= Q_3^*(0, r) = -\frac{1}{4}r + \frac{1}{4}, \\ Q_2^*(0, r) &= \frac{r}{2}. \end{aligned} \quad (23)$$

Let us move onto (20) into which we substitute (23), leading to

$$\tanh 2(-\mu_1 + \mu_3) = \frac{-r^2 - 10r + 3}{(r+3)(1-r)} =: \theta(r). \quad (24)$$

Since  $-1 < \tanh 2(-\mu_1 + \mu_3) < 1$  should hold,  $r$  satisfies  $0 < r < r_0 = -3 + 2\sqrt{3}$  due to  $\lim_{r \rightarrow 0} \theta(r) = 1$  and  $\lim_{r \rightarrow r_0} \theta(r) = -1$ . Thus, it turns out that (23) as the stationary solution is valid only for  $0 < r < r_0$ . Note that  $\lim_{r \rightarrow 0} Q_1^*(0, r) = \sup Q_1^*(0, 0) = \frac{3}{4}$ ,  $\lim_{r \rightarrow 0} Q_3^*(0, r) = \inf Q_3^*(0, 0) = \frac{1}{4}$ , and  $\lim_{r \rightarrow 0} Q_2^*(0, r) = Q_2^*(0, 0) = 0$  hold.

Next, among the other 5 possibilities of taking values of  $G_\beta^{(1)}$  and  $G_\beta^{(3)}$ , when the following two conditions

$$\begin{cases} -2Q_1^* + 2Q_3^* + 1 < 0, \\ 2Q_1^* - 2Q_3^* + 1 > 0, \end{cases} \quad (25)$$

hold, based on (4) we obtain

$$\begin{aligned} & -\frac{1}{2}(1-r)Q_1^* + r(1-Q_1^*) = 0, \\ & \frac{1}{2}(1-r)(1-Q_1^* - Q_3^*) - rQ_3^* = 0, \end{aligned} \quad (26)$$

where we have used

$$\lim_{T \rightarrow 0} G_\beta^{(1)}(Q_3^* - Q_1^*) = -1, \quad (27)$$

$$\lim_{T \rightarrow 0} G_\beta^{(3)}(Q_3^* - Q_1^*) = 1. \quad (28)$$

It reads

$$\begin{aligned} Q_1^*(0, r) &= \frac{2r}{1+r}, \\ Q_3^*(0, r) &= \frac{(1-r)^2}{(1+r)^2}, \\ Q_2^*(0, r) &= \frac{2r(1-r)}{(1+r)^2}. \end{aligned} \quad (29)$$

Substituting (29) into the two conditions of (25) gives

$$\begin{cases} 3r^2 + 10r - 1 > 0, \\ r^2 + 6r - 3 > 0, \end{cases}$$

which lead to  $r_0 < r \leq 1$ . Thus, the obtained solution (29) is valid only for  $r_0 < r \leq 1$ . Combining two cases of smaller  $r$  and larger  $r$  than  $r_0$ , the left-sided limit and the right-sided limit of  $Q_h^*$  as  $r \rightarrow r_0$  coincide. Note that the other 4 cases for the possibilities of taking values of  $G_\beta^{(h)}(a)$  give no solutions of equation (4).

In order to compute the response  $\mu_h(0, r)$ , we can perform Taylor series expansion as

$$Q_h^*(T, r) = Q_h^*(0, r) + \mu_h(0, r)T + O(T^2). \quad (30)$$

Substituting this form into (4) with (22) for  $0 < r < r_0$ , we obtain, up to  $O(T)$  order,

$$\begin{aligned} \frac{(1-r)}{4}(1 - Q_1^* - Q_3^*) &\left\{ 1 + \tanh 2(-\mu_1 + \mu_3 + O(T)) \right\} \\ - \frac{(1-r)}{4}Q_1^* &\left\{ 1 - \tanh 2(-\mu_1 + \mu_3 + O(T)) \right\} + r(1 - Q_1^*) = 0, \end{aligned} \quad (31)$$

$$(1-r)\mu_1 + (1+r)\mu_3 = 0. \quad (32)$$

Note that the first equation does not give an explicit exact solution up to  $O(T)$  order.

Combining (32) with (24), we obtain

$$\begin{aligned} \mu_1(0, r) &= -\frac{1+r}{4} \operatorname{artanh} \theta(r), \\ \mu_3(0, r) &= \frac{1-r}{4} \operatorname{artanh} \theta(r). \end{aligned} \quad (33)$$

Note that  $\mu_2 = -\mu_1 - \mu_3$  holds by definition, leading to

$$\mu_2(0, r) = \frac{r}{2} \operatorname{artanh} \theta(r). \quad (34)$$

Thus, it turns out that  $|\mu_h| \simeq \log(r - r_0)$  for each  $h$ .

Let us move onto the case of  $r_0 < r \leq 1$ . By using the same Taylor series expansion, instead of (31), we obtain

$$-r\mu_1 - \frac{1}{2}(1-r)\mu_1 = 0. \quad (35)$$

Then, combining this equation with (32) leads to

$$\mu_1(0, r) = \mu_3(0, r) = \mu_2(0, r) = 0. \quad (36)$$

### C. The explicit expressions of $Q_h^*$ and $\nu_h$ at $\beta \rightarrow 0$

Based on (4), taking into account

$$\lim_{\beta \rightarrow 0} G_\beta^{(h)}(a) = 0, \quad (37)$$

we obtain the following:

$$\begin{aligned} \frac{(1-r)}{4}(1 - Q_1^* - Q_3^*) - \frac{(1-r)}{4}Q_1^* + r(1 - Q_1^*) &= 0, \\ \frac{(1-r)}{4}(1 - Q_1^* - Q_3^*) - \frac{(1-r)}{4}Q_3^* - rQ_3^* &= 0. \end{aligned} \quad (38)$$

Solving these equations, we obtain

$$\begin{aligned} Q_1^*(\infty, r) &= \frac{5r^2 + 10r + 1}{3r^2 + 10r + 3}, \\ Q_3^*(\infty, r) &= \frac{(1-r)^2}{3r^2 + 10r + 3}, \\ Q_2^*(\infty, r) &= \frac{-3r^2 + 2r + 1}{3r^2 + 10r + 3}, \end{aligned} \quad (39)$$

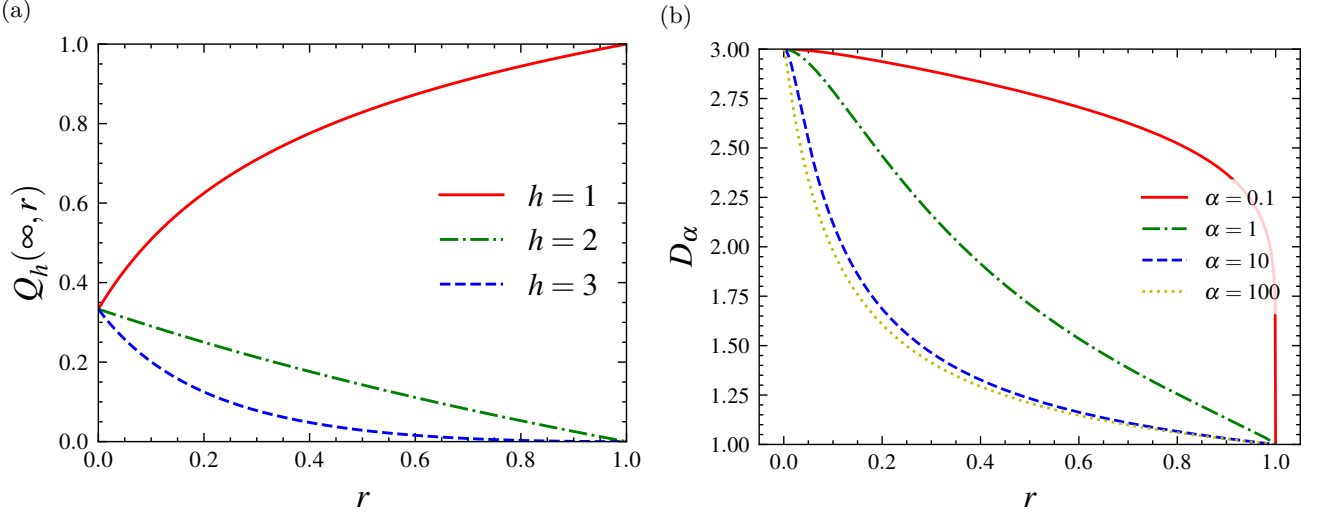


FIG. 1: (a)  $Q_h^*$  as a function of  $r$  for  $T = \infty$ . (b)  $D_\alpha$  as a function of  $r$  for  $T = \infty$ .

which are shown in Fig. 1(a).

In order to compute the response  $\nu_h(T, r) := \frac{\partial Q_h^*}{\partial \beta}$ , we perform Taylor series expansion of  $Q_h^*(T, r)$  at  $T = \infty$  as

$$Q_h^*(T, r) = Q_h^*(\infty, r) + \nu_h(\infty, r)\beta + O(\beta^2). \quad (40)$$

Substituting this form into (4), we obtain

$$\begin{aligned} -\frac{1-r}{4}(\nu_1 + \nu_3) - \frac{1-r}{4}\nu_1 - r\nu_1 &= 0, \\ -\frac{1-r}{4}(\nu_1 + \nu_3) - \frac{1-r}{4}\nu_3 - r\nu_3 &= 0. \end{aligned} \quad (41)$$

Solving these equations, we obtain

$$\nu_1 = \nu_3 = 0, \quad (42)$$

leading to  $\nu_2 = 0$  by definition.

Note that by taking the derivative of the stationary solutions from (39) with respect to  $r$ , we also have

$$\chi_1(\infty, 0) = \frac{20}{9}, \quad (43)$$

$$\chi_3(\infty, 0) = -\frac{16}{9}, \quad (44)$$

$$\chi_2(\infty, 0) = -\frac{4}{9}, \quad (45)$$

which are consistent with the expression of (17) in the limit of  $\beta \rightarrow 0$ .

## II. HILL NUMBERS $D_\alpha(r)$ AS A FUNCTION OF $r$

Let us define  $M_\alpha := \log D_\alpha$  and  $\mathbf{Q}^* := (Q_1^*, Q_2^*, Q_3^*) \in [0, 1]^3$ . Then, the sign of  $\partial_r M_\alpha$  is the same as that of  $\partial_r D_\alpha$ . Indeed, we get the following:

$$\partial_r M_\alpha = \alpha(1 - \alpha)^{-1} \left( \sum_h (Q_h^*)^\alpha \right)^{-1} F_\alpha(\mathbf{Q}^*), \quad (46)$$

$$F_\alpha(\mathbf{Q}^*) = \sum_h (Q_h^*)^{\alpha-1} \chi_h. \quad (47)$$

Thus, the nontrivial part determining the sign of  $\partial_r D_\alpha$  is  $F_\alpha$ , which has key information to find out the local maximum point  $r_\ell(T, \alpha)$  of  $D_\alpha$ . Note that  $F_\alpha = 0$  at  $\alpha = 1$  holds due to  $\sum_h \chi_h = 0$ .

### A. The existence of a local maximum of $D_\alpha$ at $T \rightarrow 0$ for any $0 < \alpha < \infty$

First, let us consider the case of  $r < r_0$  and  $T \rightarrow 0$  where we use equations (23) by putting  $r = r_0$ . Then, as shown in Fig. 2(a), we obtain that  $F_\alpha < 0$  for  $\alpha > 1$ ,  $F_\alpha > 0$  for  $0.199 \leq \alpha < 1$ , and  $F_\alpha < 0$  for  $\alpha \leq 0.198$  as  $r \rightarrow r_0$ . It means that for  $\alpha \geq 0.199$ ,  $\partial_r D_\alpha$  as  $r \rightarrow r_0$  is positive, whereas it is negative for  $0 < \alpha \leq 0.198$ .

Second, let us consider the case of  $r > r_0$  where we use equations (29) by putting  $r = r_0$ . Then, as shown in Fig. 2(b), it turns out that  $F_\alpha > 0$  for  $\alpha > 1$  and  $F_\alpha < 0$  for  $\alpha < 1$ . It means that  $\partial_r D_\alpha$  as  $r \rightarrow r_0$  is negative for any  $\alpha > 0$ .

Therefore, combining two cases together, we reach the conclusion that there is a local maximum point  $r_\ell(0, \alpha) > 0$  at  $T \rightarrow 0$  for any  $\alpha > 0$ . The concrete values of  $r_\ell(0, \alpha)$  are  $r_0$  for  $\alpha \geq 0.199$ , and get smaller than  $r_0$  between  $\alpha = 0.198$  and  $0.199$ . Then,  $\lim_{\alpha \rightarrow 0} r_\ell(0, \alpha)$  is numerically estimated as  $0.451 \dots$ .

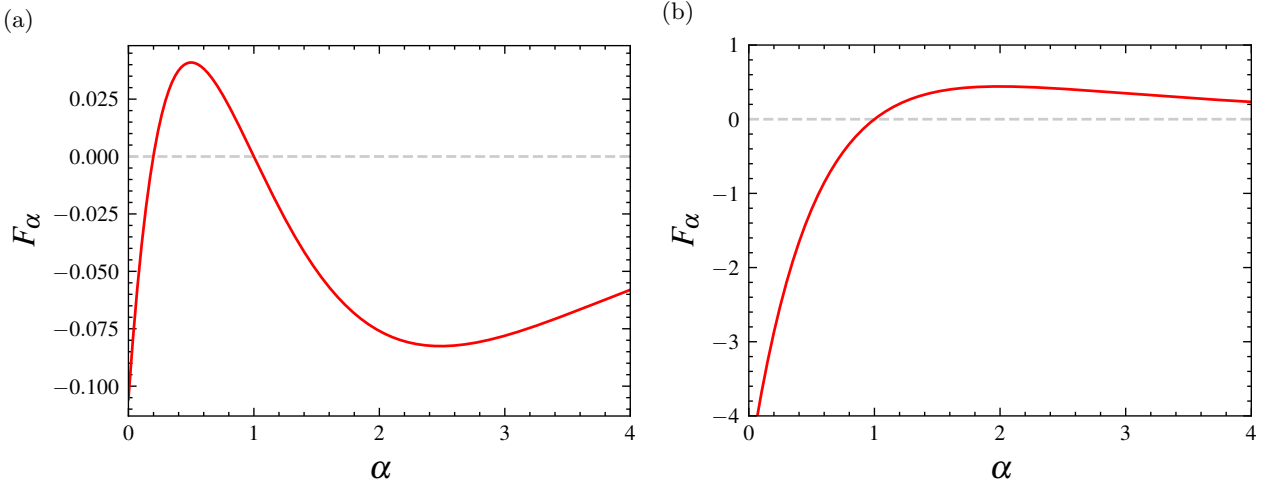


FIG. 2: (a)  $\lim_{r \rightarrow r_0} F_\alpha$  as a function of  $\alpha$  for  $r < r_0$ . (b)  $\lim_{r \rightarrow r_0} F_\alpha$  as a function of  $\alpha$  for  $r > r_0$

### B. The absence of local maxima of $D_\alpha$ at $T \rightarrow \infty$ for $0 < \alpha < \infty$

Suppose the following condition that for a fixed  $T$ ,  $\chi_1 > 0$ ,  $\chi_2 < 0$ ,  $\chi_3 < 0$ , and  $Q_1^* > Q_2^*, Q_3^*$  hold for  $0 < r \leq 1$ . On that condition, we can derive that  $(Q_1^*)^{\alpha-1}\chi_1$  as a term in  $F_\alpha$  can be larger than  $|(Q_2^*)^{\alpha-1}\chi_2 + (Q_3^*)^{\alpha-1}\chi_3|$  for  $\alpha > 1$ , and smaller than it for  $0 < \alpha < 1$ . This leads to that for  $0 < r \leq 1$ ,  $F_\alpha > 0$  holds for  $\alpha > 1$ , and  $F_\alpha < 0$  holds for  $0 < \alpha < 1$ , corresponding to that there is no local maximum of  $D_\alpha$  as a function of  $r$  in  $0 < r \leq 1$  for  $\alpha > 0$ .

The derivation of the above conclusion is as follows. First, it is straightforward to see

$$\begin{aligned} |(Q_2^*)^{\alpha-1}\chi_2 + (Q_3^*)^{\alpha-1}\chi_3| &= (Q_2^*)^{\alpha-1}\chi_1 + (Q_3^*)^{\alpha-1}|\chi_3| - (Q_2^*)^{\alpha-1}|\chi_3| \\ &= (Q_3^*)^{\alpha-1}\chi_1 + (Q_2^*)^{\alpha-1}|\chi_2| - (Q_3^*)^{\alpha-1}|\chi_2|, \end{aligned} \quad (48)$$

where we have used  $\sum_h \chi_h = 0$ . Hence, we obtain

$$\chi_1 \min(Q_2^*, Q_3^*)^{\alpha-1} \leq |(Q_2^*)^{\alpha-1}\chi_2 + (Q_3^*)^{\alpha-1}\chi_3| \leq \chi_1 \max(Q_2^*, Q_3^*)^{\alpha-1}. \quad (49)$$

It means that for  $\alpha > 1$ , the following holds:

$$\chi_1(Q_1^*)^{\alpha-1} > \chi_1 \max(Q_2^*, Q_3^*)^{\alpha-1}, \quad (50)$$

which immediately leads to  $F_\alpha > 0$ . On the other hand, for  $0 < \alpha < 1$ , the following holds:

$$\chi_1(Q_1^*)^{\alpha-1} < \chi_1 \min(Q_2^*, Q_3^*)^{\alpha-1}, \quad (51)$$

which immediately leads to  $F_\alpha < 0$ . Thus, we reach the conclusion mentioned above.

For  $T = \infty$ , (39) directly means that the conditions of  $\chi_1 > 0$ ,  $\chi_2 < 0$ ,  $\chi_3 < 0$ , and  $Q_1^* > Q_2^*, Q_3^*$  hold. Thus, it leads to the absence of local maxima of  $D_\alpha$  in  $0 < r \leq 1$  for any  $\alpha > 0$  as shown in Fig. 1(b).

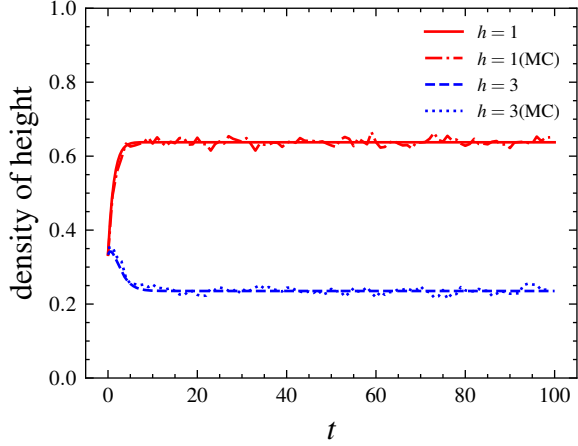


FIG. 3: The Monte Carlo (MC) simulation with  $N = 1000$  and the solutions of the population dynamics (1).  $T = 1$ ,  $r = 0.2$ .

Note that the conditions mentioned above can be broken, in particular, for sufficiently small  $T$ , for which the above results are not applied. Nevertheless, using a nullcline method to compute the stationary solutions of (4), we have numerically estimated that there is  $\alpha_0(T) > 0$  such that for  $\alpha > \alpha_0(T)$ , there are no local maxima of  $D_\alpha$  for  $T \geq 0.26$ , whereas for  $T \leq 0.25$ , there is a local maximum of  $D_\alpha$  for any  $\alpha > 0$ .

### III. MONTE CARLO SAMPLING

#### A. Updating rules

Let us explain how to obtain sample trajectories by Monte Carlo simulations and compare them with the solutions of the derived population dynamics (1). As Monte Carlo simulations, we perform the following procedures:

Initially, prepare a configuration  $\mathbf{x}$  where the state at each site is a value taken randomly from  $\{1, 2, 3\}$  with uniform distribution. That is, the probability of taking each state is  $1/3$ .

Next, repeat the steps from 1 to 3:

1. Choose randomly a name  $\ell$  ( $1 \leq \ell \leq N$ ) of an agent with uniform distribution. That is, the probability of taking each name is  $1/N$ .
2. With the probability  $r$ , the chosen agent  $\ell$  is disturbed, making the transition from state  $x_\ell$  to 1.
3. If the chosen agent  $\ell$  is not disturbed, choose either positive or negative direction with probability  $1/2$ .
  - (a) If positive direction is chosen and  $x_\ell \neq 3$ , make the transition from state  $x_\ell$  to  $x_\ell + 1$  with the probability

$$\frac{1}{2} \left( 1 + \tanh \beta \left( 2(x_\ell - \frac{1}{N} \sum_{k \neq \ell} x_k) + 1 \right) \right). \quad (52)$$

- (b) If negative direction is chosen and  $x_\ell \neq 1$ , make the transition from state  $x_\ell$  to  $x_\ell - 1$  with the probability

$$\frac{1}{2} \left( 1 + \tanh \beta \left( -2(x_\ell - \frac{1}{N} \sum_{k \neq \ell} x_k) + 1 \right) \right). \quad (53)$$

As shown in Fig. 3, we have confirmed that Monte Carlo simulations have good agreement with the solution of the population dynamics (1).

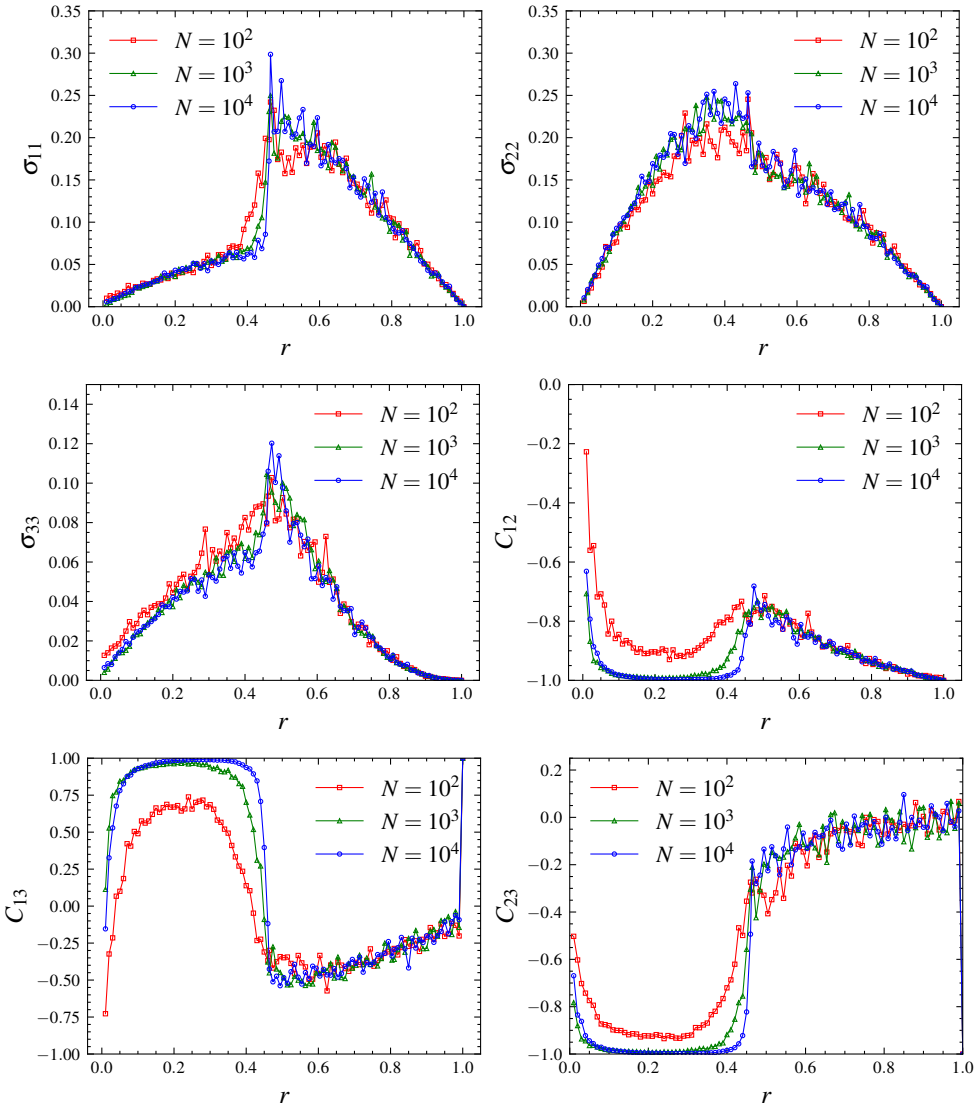


FIG. 4: The variance  $\sigma_{hh}$  and correlation coefficients  $C_{hh'}$  averaged over 10 samples with different trajectories.  $T = 10^{-3}$ ,  $t_0 = 100$ ,  $\tau = 150$ ,  $N = 10^2, 10^3, 10^4$ .

## B. Finite-size fluctuations

Let us characterize the finite size fluctuations in the density of each state by variance  $\sigma_{hh}$ , covariance  $\sigma_{hh'}$ , and correlation coefficient  $C_{hh'}$  for  $h, h' \in \{1, 2, 3\}$ , which are defined as

$$\sigma_{hh'} := \frac{N}{\tau - t_0} \sum_{t=t_0}^{\tau} \Delta_h(t) \Delta_{h'}(t), \quad (54)$$

$$\Delta_h(t) := \hat{Q}_h(t) - Q_h^*, \quad (55)$$

$$C_{hh'} := \frac{\sigma_{hh'}}{\sqrt{\sigma_{hh}} \sqrt{\sigma_{h'h'}}}, \quad (56)$$

where  $\hat{Q}_h(t)$  is a sample trajectory of density of state  $h$  obtained from Monte Carlo simulation at time  $t$ . The time unit is one Monte Carlo step per site ( $N$  steps). We set  $t_0 = 100$  because the typical trajectories of  $\hat{Q}_h(t)$  with  $r \geq 10^{-2}$  and  $T = 10^{-3}$  crosses the stationary solution much before  $t = t_0 = 100$ . Indeed, for  $r \leq 10^{-3}$  and  $T = 10^{-3}$ , the dynamics gets very slow and the typical trajectories do not cross the stationary solutions by  $t = t_0 = 100$ .

As shown in Fig. 4, we have performed Monte Carlo simulations with different systems size  $N$ . If we straightforwardly extrapolate the behaviors for larger system size, there seem to be singular behaviors in the three types of variance and the three types of correlation function in the large size limit near  $r = r_0$  for  $r < r_0$ . In particular, it is notable to point out that three correlation coefficients in the large size limit seem to have perfect correlation, corresponding to  $|C_{hh'}| = 1$ , for only  $r < r_0$ .

Thus, the results obtained by Monte Carlo simulations suggest that there is a universal curve presumably independent of  $N$ . Further, in the larger system sizes, it is more obvious that  $C_{hh'}$  for  $r < r_0$  show U-shaped curves. It is notable that the bottoms of the U-shaped curves are close to  $r = -5 + 2\sqrt{7} \simeq 0.291 \dots$ , which is the point where  $\mu_h$  changes its sign. Nevertheless, more works with sufficiently large samples need to be done to obtain more convincing data, which remain to be found as another work in the future.